biology letters

rsbl.royalsocietypublishing.org

Research

Cite this article: Wang Y, Srinivasan M. 2014 Stepping in the direction of the fall: the next foot placement can be predicted from current upper body state in steady-state walking. *Biol. Lett.* **10**: 20140405.
http://dx.doi.org/10.1098/rsbl.2014.0405

Received: 21 May 2014
Accepted: 1 September 2014

Subject Areas:
biomechanics, neuroscience, bioengineering

Keywords:
biomechanics, foot placement, walking, stability, control, dynamics

Author for correspondence:
Manoj Srinivasan
e-mail: srinivasan.88@osu.edu

Electronic supplementary material is available at http://dx.doi.org/10.1098/rsbl.2014.0405 or via http://rsbl.royalsocietypublishing.org.

Royal Society Publishing

Stepping in the direction of the fall: the next foot placement can be predicted from current upper body state in steady-state walking

Yang Wang and Manoj Srinivasan

Mechanical and Aerospace Engineering, The Ohio State University, Columbus, OH 43210, USA

During human walking, perturbations to the upper body can be partly corrected by placing the foot appropriately on the next step. Here, we infer aspects of such foot placement dynamics using step-to-step variability over hundreds of steps of steady-state walking data. In particular, we infer dependence of the 'next' foot position on upper body state at different phases during the 'current' step. We show that a linear function of the hip position and velocity state (approximating the body center of mass state) during mid-stance explains over 80% of the next lateral foot position variance, consistent with (but not proving) lateral stabilization using foot placement. This linear function implies that a rightward pelvic deviation during a left stance results in a larger step width and smaller step length than average on the next foot placement. The absolute position on the treadmill does not add significant information about the next foot relative to current stance foot over that already available in the pelvis position and velocity. Such walking dynamics inference with steady-state data may allow diagnostics of stability and inform biomimetic exoskeleton or robot design.

1. Introduction

Humans use active neuromuscular control to stabilize their top-heavy bodies during walking [1]. Mathematical models [1–3] suggest the effectiveness of appropriate foot placement to avoid falling forward or sideways: a person falling rightwards could produce a corrective leftward force effectively by placing the next foot to the right of its usual position. Experiments involving external mechanical [3] and visual perturbations [4] have found some evidence for such foot placement dynamics, likely due to both active control and passive dynamics. In this article, we infer plausible foot placement dynamics without such external perturbations, using natural step-to-step variability in steady-state walking data; see figure 1*a* for foot placement variability. Such natural variability might contain stabilizing responses to internal muscle and sensory noise [5–7]. Exploiting such variability [5–7], we infer how the foot position depends on the state of the upper body (pelvis) state during the previous step, explaining a large fraction of the random-looking variability in figure 1*a*.

2. Material and methods

(a) Experimental

Subjects gave informed consent. Subjects ($N = 10$, eight male, two female, age 27.50 $\pm$ 5.10 years, height 1.74 $\pm$ 0.11 m, body mass 76.8 $\pm$ 14.2 kg; mean $\pm$ s.d.) walked on a treadmill for 5 min each at three constant speeds: at 1.0, 1.2 and 1.4 m s^{-1} for five subjects and at 0.98, 1.25 and 1.43 m s^{-1} for the rest, averaging 265 strides per trial (s.d. 36). Walking motions were recorded using a marker-based motion capture system (Vicon T20, position error < 0.3 mm), with four markers on each foot including an ankle

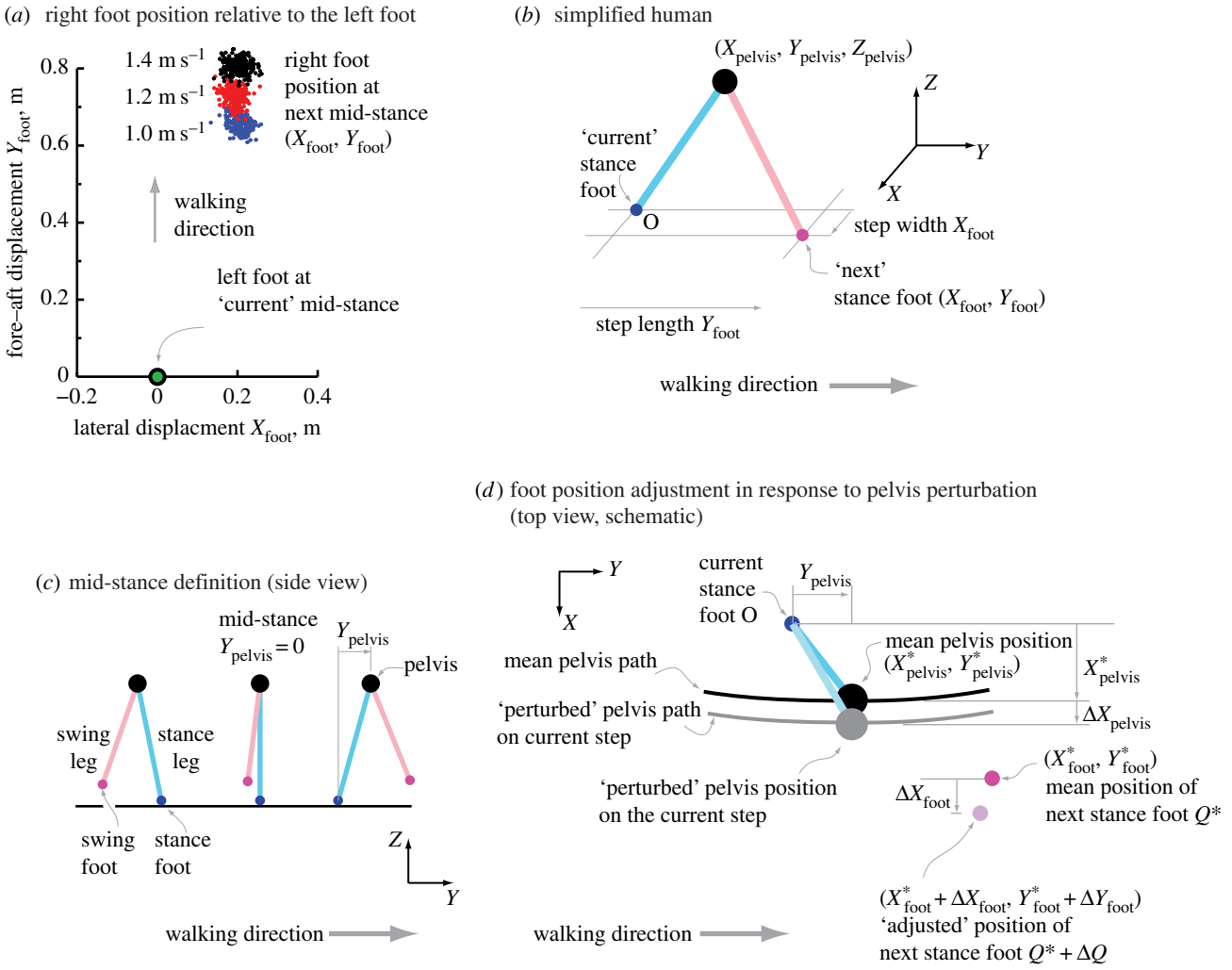

Figure 1. Describing walking motion with pelvis and foot positions. (*a*) The right-foot position at mid-stance relative to the previous left-foot stance position, shown for a single subject, for each of about 265 strides at 1 m s^{-1} (blue dots), 1.2 m s^{-1} (red) and 1.4 m s^{-1} (black). (*b*) Human walking motion represented by pelvis position and two foot positions. (*c*) Mid-stance is defined as when the swing foot has the same fore–aft position as the pelvis. The stance foot position is assumed fixed at the foot position at mid-stance. (*d*) A schematic showing a deviation from the average pelvis trajectory and a corresponding change in the next stance foot position.

marker and three markers on the upper pelvic region, close to the level of the body center of mass (see the electronic supplementary material for marker locations). No forces were measured.

(b) Describing the walking motion with pelvis and foot positions

For simplicity, we represent human walking in three dimensions by three salient points (figure 1*b*): one for the 'pelvis', a weighted sum of the three markers approximating the body centre of mass (see the electronic supplementary material), and one for each foot (ankle). Here, Y is fore–aft, X is lateral (sideways and rightwards) and Z is vertical. These axes do not rotate relative to the ground. Figure 1*b* shows the pelvis position $(X_{\text{pelvis}}, Y_{\text{pelvis}}, Z_{\text{pelvis}})$ and the position of the 'next' stance foot $(X_{\text{foot}}, Y_{\text{foot}}, 0)$, measured relative to the position of the 'current' stance foot (origin O). We define 'mid-stance' of each stance phase as when the pelvis has the same fore–aft position as the stance foot (figure 1*c*). During each stance phase, the current stance foot (origin O) is considered fixed at its mid-stance value and travels with the treadmill belt. Thus, mid-stance is $Y_{\text{pelvis}} = 0$. We normalize the 'distance from mid-stance' Y_{pelvis} by the trial's mean stride length D_{stride} to obtain $\phi = Y_{\text{pelvis}}/D_{\text{stride}}$, a proxy for the 'phase' of the system along the gait cycle. If $\phi = 0$ is a left mid-stance, the next right mid-stance is around $\phi = +0.5$. The swing foot is the foot contralateral to the current stance foot (figure 1*c*) and eventually becomes the next stance foot.

(c) Inferring foot placement dynamics

During each step, the pelvis state $P(\phi)$ as a function of distance from mid-stance ϕ is

$$P(\phi) = (X_{\text{pelvis}}(\phi), Z_{\text{pelvis}}(\phi), \dot{X}_{\text{pelvis}}(\phi), \dot{Y}_{\text{pelvis}}(\phi), \dot{Z}_{\text{pelvis}}(\phi)),$$

noting equivalence of Y_{pelvis} and ϕ. The next (contralateral) stance foot position is $Q = (X_{\text{foot}}, Y_{\text{foot}})$. For each trial, $P^*(\phi)$ and Q^* are averages of these quantities over all strides.

Given pelvis state $P(\phi)$, we wish to predict the next foot position Q (figure 1*d*). We seek a linear relation between the deviation from the mean pelvis state $\Delta P(\phi) = P(\phi) - P^*(\phi)$ and the deviation from the mean foot position $\Delta Q = Q - Q^*$

$$\Delta Q = J(\phi)\,\Delta P(\phi). \tag{2.1}$$

Here, $J(\phi)$ is a 2×5 matrix, the partial derivative (sensitivity or Jacobian or regression coefficients matrix) of the foot position with respect to the pelvis state $P(\phi)$, for example, the (1, 1) element of $J(\phi)$ is $\partial X_{\text{foot}}/\partial X_{\text{pelvis}}(\phi)$. The elements have units consistent with displacements in metres and time in seconds. Each trial of steady human walking gives $P(\phi)$ and Q for hundreds of strides. We estimate $J(\phi)$ by ordinary least squares (electronic supplementary material).

We also obtained linear relations between other sets of input and output variables, for instance, including additional input variables such as swing foot position and velocity (denoted $R(\phi)$) or the absolute position of the person on the treadmill,

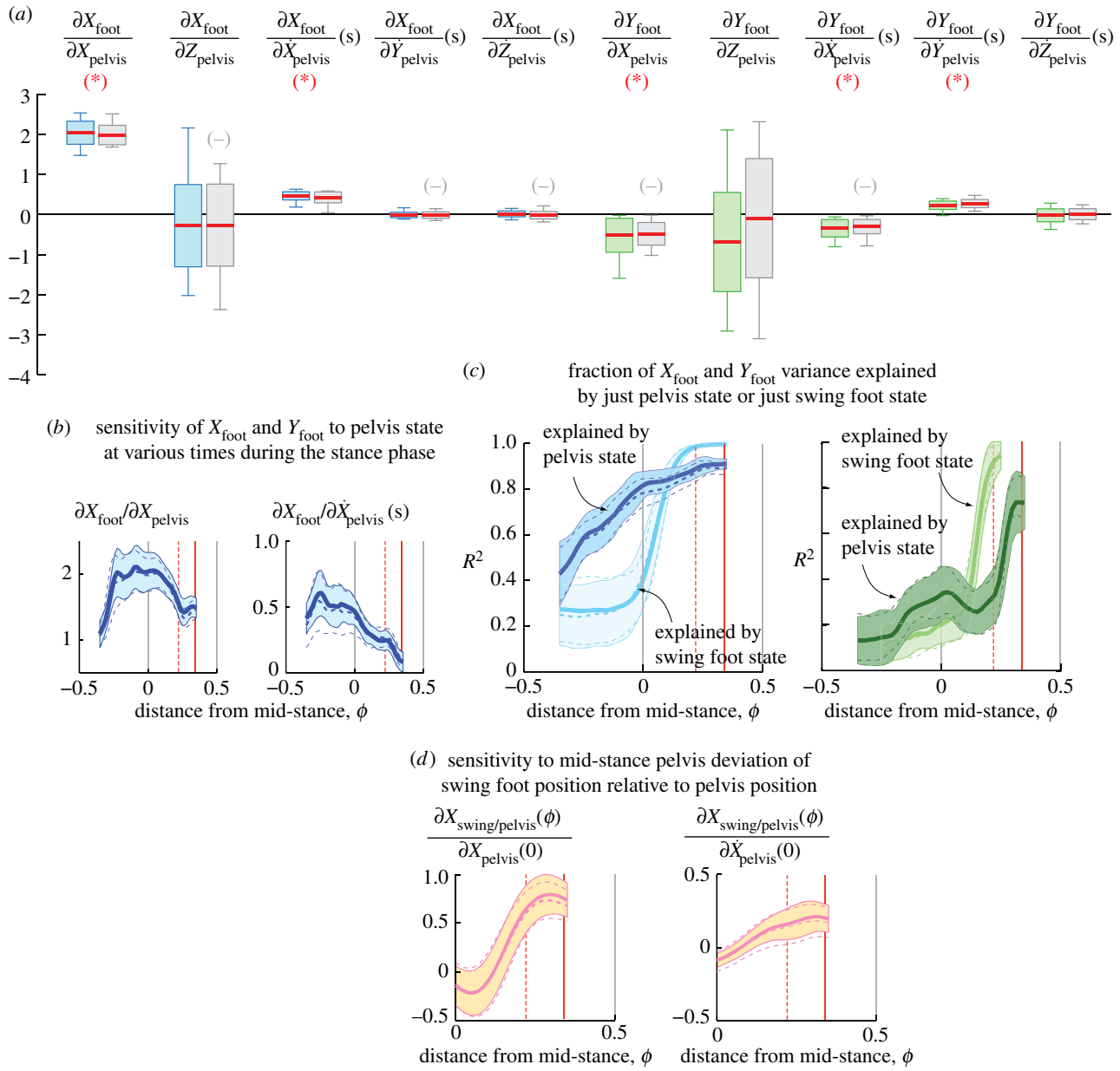

Figure 2. Foot placement dynamics. (*a*) The estimated partial derivative $J(0)$ of the foot position with respect to pelvis state at mid-stance $P(0)$; box-plot shows mean across subjects and trials (red midline), standard deviation over all trials (boxes) and 95% interval (whiskers, 2.5 to 97.5 percentile). Colour shading indicates left to right transitions and grey indicates right to left. A negative sign (−) indicates display of the sign-reversed coefficients for some right to left transitions; red asterisks indicate coefficients statistically different from zero ($p < 0.05$). (*b*) Sensitivity of foot position on selected pelvis states at different phases ϕ; mean (thick solid line) $\pm$ s.d. (coloured band) are shown for left to right transitions; see the electronic supplementary material, figure S4. (*c*) Fraction of foot position variance explained by phase-dependent pelvis state (dark colours) or the phase-dependent swing foot state (light colours). (*d*) The sensitivity of the swing foot relative to the pelvis, in response to mid-stance pelvis deviations. In panels (*b–d*), red dashed ($\phi = 0.22$) and solid ($\phi = 0.34$) lines roughly indicate, respectively, moments just before heel-strike and just after push-off, with double stance between; solid lines and filled bands are for left to right transitions and dashed lines are for right to left transitions.

to see whether these variables improve predictive power (see the electronic supplementary material).

3. Results

(a) Step in the direction of the fall

Figure 2*a* shows the estimated elements of the matrix $J(0)$, relating the mid-stance pelvis state $P(0)$ to the next foot position (X_{foot}, Y_{foot}), pooled over subjects and speeds. The $J(0)$ elements did not show significant speed dependence (electronic supplementary material, figure S1). Five out of 10 elements of $J(0)$ are significantly different from zero, with their 95% CI bounded away from zero. Surrogate data analysis (electronic supplementary material, figures S2 and S3) performed by shuffling the input data sequence for given output sequence showed that these non-zero coefficients were significant at $p = 0.05$.

Using only the significantly non-zero $J(0)$ elements, we find that the sideways foot position X_{foot} is mainly affected by sideways pelvis position and velocity

$$\Delta X_{foot} \approx 2.01 \cdot \Delta X_{pelvis}(0) + 0.444 \cdot \Delta \dot{X}_{pelvis}(0). \quad (3.1)$$

Thus, in response to an extra rightward pelvis deviation (falling rightwards), the subject will step more to the right than usual, thereby stepping in the direction of the fall. Specifically, equation (3.1) predicts that deviations of 1 cm and

1 cm s^{-1} in rightward hip position and speed, respectively, will result in a 2.45 cm rightward deviation of the next stance foot. Equation (3.1) applies to transitions from left to right stance or vice versa.

Analogously, the forward foot position Y_{foot} is

$$\Delta Y_{foot} \approx -0.52 \cdot \Delta X_{pelvis} - 0.34 \cdot \Delta \dot{X}_{pelvis} + 0.23 \cdot \Delta \dot{Y}_{pelvis}. \quad (3.2)$$

This expression corresponds to transitions from left to right stance phases: rightward pelvis perturbations during left mid-stance imply shorter right steps; larger forward speeds imply longer steps. For right to left transitions, we switch 'left' and 'right' in the previous statement; the equation is similar except for sign changes due to 'leftward' being the 'negative' X-direction: $\Delta Y_{foot} \approx +0.48 \cdot \Delta X_{pelvis} + 0.304 \cdot \Delta \dot{X}_{pelvis} + 0.27 \cdot \Delta \dot{Y}_{pelvis}$. These coefficients show approximate left–right mirror-symmetry of walking.

(b) Dependence of coefficients on distance to mid-stance

Figure 2*b* shows that the estimated $J(\phi)$ varies systematically with distance ϕ from mid-stance. In particular, the coefficients $\partial X_{foot}/\partial X_{pelvis}(0)$ and $\partial X_{foot}/\partial \dot{X}_{pelvis}(0)$ decrease with increase in ϕ beyond mid-stance. The electronic supplementary material has detailed depictions of these ϕ-dependent regression results for various input–output pairs: from pelvis state $P(\phi)$ to Q (electronic supplementary material, figure S4), from swing foot state $R(\phi)$ to Q (electronic supplementary material, figure S5) and from $(P(\phi), R(\phi))$ to Q (electronic supplementary material, figure S6). The phase-dependent linear relations (figure 2*b*; electronic supplementary material, figure S4) could provide a phase-dependent target for the foot position.

(c) Mid-stance pelvis state explains sideways foot position

The pelvis state at mid-stance explains about 81% of the next X_{foot} variance (R^2 values, figure 2*b*), almost entirely due to variables in equation (3.1). The pelvis state just before heel-strike ($\phi = 0.22$) can explain a higher fraction (89%) of the X_{foot} variance. The mid-stance pelvis state can also explain 61% of the variance of sideways foot position relative to pelvis at heel-strike. Mid-stance pelvis state explains about 33% of Y_{foot} variance.

Notably, mid-stance pelvis state explains X_{foot} variance better than the mid-stance swing foot state (81% versus 40%, figure 2*b*). Adding mid-stance swing foot state to the pelvis state as a regressor does not give us any more than 81% variance explanation (electronic supplementary material, figure S6). Thus, at mid-stance, the pelvis 'knows' much more about the future foot position than the foot itself. The swing foot becomes the next stance foot position and so, eventually overtakes the pelvis state's predictive ability (figure 2*b*). Assuming linearity, these trends suggest that most swing foot deviation typically happens after mid-stance.

Regressions from mid-stances of even earlier steps find that the Jacobian coefficients and the foot position variance fraction explained both approach zero (electronic supplementary material, figure S10). The X_{foot} variance explained is 13% instead of 81% if we used the previous ipsilateral mid-stance pelvis state.

(d) Relative motion of swing foot and pelvis

For instance, the swing foot position relative to pelvis is $(X_{swing/pelvis}, Y_{swing/pelvis})$, where $X_{swing/pelvis} = (X_{swing} - X_{pelvis})$, etc. Figure 2*d* shows that the partial derivatives of the swing-foot–pelvis separation with respect to sideways deviations are positive by heel-strike (electronic supplementary material, figure S8). Thus, while a rightward pelvis deviation at mid-stance will result in further rightward pelvis deviation between mid-stance and heel-strike, it will result in an even greater rightward deviation of the next foot position; thus, we can rule out the foot placement deviation being entirely due to the pelvis deviation with the foot being rigidly carried by the pelvis.

(e) Station-keeping: effect of position on treadmill

A treadmill's finite dimensions may affect walking dynamics: humans may wish to avoid the treadmill's edge (electronic supplementary material, figure S11). However, including the person's position on the treadmill as a regressor in addition to the pelvis state explains only 2–5% more foot position variance (electronic supplementary material, figure S9). The subjects' position on the treadmill drifts slowly and is not as well controlled as limb states relative to the body, perhaps because station-keeping is less important than not falling. These results were not affected by the substantial treadmill width differences between subjects 1–5 and 6–10 (widths 0.92 m versus 0.51 m; electronic supplementary material, figure S1).

4. Discussion

By fitting linear relations to variability in steady-state walking data, we have inferred foot placement dynamics consistent with the idea that the foot positions change in the perturbation direction. These foot position dependencies could be due to active feedback control in response to pelvis state deviations, or due to passive dynamics and feed-forward control. Thus, most conservatively, our results are only about the pelvis state's (i.e. approximate centre of mass state's) predictive ability of the next foot position. Nevertheless, we have shown that what seems 'random variability' in figure 1*a* can be explained by a simple linear function of pelvis state deviations far in advance of heel-strike. Also, the foot position dependence on state at different gait phases ϕ (figure 2*b*; electronic supplementary material, S4 and S5) provides a more general description of foot position dynamics, which could be used in a foot-position controller, say, in an exoskeleton for walking assistance.

Equations (3.1) and (3.2) are formal data-derived versions of those previously proposed [1,3]. By showing that all terms except the sideways position and velocity terms drop out of equation (3.1), our results support the assumptions in the so-called extrapolated centre of mass model [3], similar to our simple linear models but not allowing for phase-dependence and arbitrary regression; further study is necessary to distinguish which model is better. Stride length reduction in equation (3.2) may be analogous to shorter stride times in perturbation experiments [3].

Fitting a controlled mechanics-based model to the data may explain the systematic trends in regressed coefficients $J(\phi)$. Perturbation experiments could test whether inferred relations

from steady-state data can reliably predict consequences of external perturbations. Performing external perturbations [3,4] and inferring the subsequent inputs to the leg muscles (from electromyography or inverse dynamics) can delineate the relative importance of feedback and feed-forward control.

Detailed inference of human walking controller could inform diagnoses of human stability and the design of biomimetic assistive exoskeletons and walking robots. Future work on such controller inference could also consider overground experiments, longer term correlations and planning, more degrees of freedom, fits to a muscle-driven mechanics-based model and nonlinear controller models.

Ethics statement. The protocol was approved by OSU's Institutional Review Board.

Data accessibility. Data is available through Dryad (doi:10.5061/dryad.5kh00).

Funding statement. This work was supported in part by NSF grant no. 1254842.

References

1. Bauby CE, Kuo AD. 2000 Active control of lateral balance in human walking. *J. Biomech.* **33**, 1433–1440. (doi:10.1016/S0021-9290(00)00101-9)
2. Redfern MS, Schumann T. 1994 A model of foot placement during gait. *J. Biomech.* **27**, 1339–1346. (doi:10.1016/0021-9290(94)90043-4)
3. Hof AL, Vermerris SM, Gjaltema WA. 2010 Balance responses to lateral perturbations in human treadmill walking. *J. Exp. Biol.* **213**, 2655–2664. (doi:10.1242/jeb.042572)
4. O'Connor SM, Kuo AD. 2009 Direction-dependent control of balance during walking and standing. *J. Neurophysiol.* **102**, 1411. (doi:10.1152/jn.00131.2009)
5. Hurmuzlu Y, Basdogan C. 1994 On the measurement of dynamic stability of human locomotion. *J. Biomech. Eng.* **116**, 30–36. (doi:10.1115/1.2895701)
6. Dingwell JB, Cusumano JP. 2001 Local dynamic stability versus kinematic variability of continuous overground and treadmill walking. *J. Biomech. Eng.* **123**, 27–32. (doi:10.1115/1.1336798)
7. Revzen S, Guckenheimer JM. 2012 Finding the dimension of slow dynamics in a rhythmic system. *J. R. Soc. Interface* **9**, 957–971. (doi:10.1098/rsif.2011.0431)

Electronic Supplementary Information for:

Stepping in the direction of the fall: the next foot placement can be predicted from current upper body state in steady state walking

Yang Wang and Manoj Srinivasan
Mechanical and Aerospace Engineering, The Ohio State University, Columbus, OH 43210
Email: srinivasan.88@osu.edu. Web: http://movement.osu.edu

This supplementary appendix provides additional figures and other technical information supporting the main manuscript.

Linear model inference via ordinary least squares. We use ordinary least squares to infer the mapping from input to output, briefly described here. Say, on the i-th transition of a particular type (for instance, right mid-stance to next left stance foot position), the relevant input variable is C_i and the output variable is D_i, both column vectors of possibly different sizes. The proposed linear relation is $D_i = J\,C_i$ for each i. We seek the J that minimizes the sum of squared residuals

$$\sum_{i=1}^{N_{\text{strides}}} \|D_i - J\,C_i\|^2 .$$

We define $\mathbf{C} = [C_1\ C_2 \ldots]$ as a matrix consisting of the inputs for all i as columns. Similarly, $\mathbf{D} = [D_1\ D_2 \ldots]$ consists of outputs for all i as columns. Then, in `MATLAB`, the least squares estimate of J is given simply by the following expressions, all equivalent:

$$J = \mathbf{D}/\mathbf{C} = (\mathbf{D}^T \backslash \mathbf{C}^T)^T = ((\mathbf{C}^T)^\dagger \mathbf{D}^T)^T,$$

where the superscript † indicates a Moore-Penrose pseudo-inverse [1].

Bootstrap statistics. To obtain error estimates for each element of the least squares estimate J, we use bootstrap statistics [2, 3, 4]. That is, we constructed data sets consisting of the same number of strides, obtained by sampling with replacement from the strides in the original data set. This new dataset is called a bootstrap sample, from which we can again estimate J. By considering a sufficiently large number of bootstrap samples, we obtain a distribution for J, providing an estimate of the error covariances for the elements of J. The standard deviations in Figure 2a of the main manuscript represent the inter-subject and inter-trial variability of the best-fit elements of $J(0)$ from the 30 walking trials. On the other hand, Figure S2 here shows mean and standard deviation for each element of $J(0)$ by pooling the bootstrap distributions for all 30 trials.

It unclear why some coefficients have higher inter-subject and inter-trial variability whereas other coefficients have very small inter-subject and inter-trial variability (Figure 2a of main manuscript). We hypothesized that the bootstrap error estimate will also be correspondingly higher for those coefficients for which the best estimates show the greatest inter-subject and inter-trial variability. In figure S12, we plot the standard deviation of the subject-trial-variability for each coefficient versus the boot-strap error estimate for that coefficient for all subject trials; we do see that the coefficients that have high inter-subject variability also have higher error estimate for each trial (although this relation is not 1:1).

Surrogate data analysis by random shuffling and resampling. Consider a null hypothesis that the variability in the foot placement is not related to the pelvis state variability, and that any non-zero elements of

J were obtained just by chance given this null hypothesis. To test this premise, we construct surrogate data sets [5], in which the pelvis state of the i-th stride are matched with the foot position corresponding to a randomly chosen stride. In other words, we construct a new matrix $\overline{\mathbf{D}}$ whose columns are obtained by resampling the columns of $\mathbf{D}$ with replacement (simple permutations also give similar results). We estimate the corresponding J for many such surrogate datasets using ordinary least squares. The distribution of J's we obtain from such inference, shown in Figure S3, is vastly different from that obtained with the original dataset. In particular, the distribution for each coefficient from the surrogate data is more or less centered about zero. Comparing this figure to that obtained from the original data, Figure S1, we see that the 95% confidence intervals of the coefficients from the surrogate data do not overlap the best-fit non-zero $J(0)$ from the original data — implying that the probability of obtaining those non-zero elements by random chance is less than 0.05 ($p = 0.05$).

Dependence of the regressions on distance ϕ from mid-stance. In the main manuscript and in this supplementary information, a number of figures show how the regressed coefficients change when either the input variables or the output variables depend on ϕ, the distance from mid-stance.

For instance, how well the pelvis deviation at mid-stance explains future pelvis deviations (at higher ϕ) is shown in Figure S7. In particular, we see that $\partial X_{\text{pelvis}}(\phi)/\partial X_{\text{pelvis}}(0) > 0$ for $\phi > 0$; this might explain why, in Figure 2b of the main manuscript and Figure S4 here, we have $\partial X_{\text{foot}}/\partial X_{\text{pelvis}}(0) > \partial X_{\text{foot}}/\partial X_{\text{pelvis}}(\phi)$.

For such figures, the regression for each ϕ is performed independently — that is, independent of the data at neighboring ϕ. Any correlations between the state deviations from mean state at one ϕ and another are ignored. It may be that some ϕ-dependent trends in the regressed coefficients are due to such correlations and we have not ruled out this possibility.

We also performed regressions using other other phase-like variables, instead of $\phi = Y_{\text{pelvis}}/D_{\text{stride}}$. For instance, when we used normalized time, t/T_{stride}, gave essentially the same results and trends for the phase dependence of the coefficients.

Comparing different regressions: Explaining foot position with just pelvis state or just swing foot state or both. In this supplementary information and more briefly in the main manuscript, we have displayed regression from pelvis state to next foot position (Figure 2b-c, main manuscript and Figure S4 here) and from swing foot state to the next foot position (Figure 2c, main manuscript and Figure S5 here).

As expected, when we use pelvis state and swing foot state together $[P(\phi);\ R(\phi)]$ as regressors, we find that a higher fraction of the foot position variance is explained (Figure S6). More significantly, the coefficients obtained for this regression have somewhat different trends from those obtained when only pelvis state $P(\phi)$ is the regressor or only the swing foot state $R(\phi)$ is the regressor: compare Figure S6 with the corresponding coefficients in Figures S4 and S5. The differences in coefficients indicate multi-collinearity of the regressors – that is, that the pelvis state and the swing foot state might have non-trivial correlations (which, in fact, has been the subject of this paper).

Around mid-stance, the coefficients for the pelvis state are similar in Figure S4 and Figure S6 — suggesting that at mid-stance, the pelvis state is the dominant explainer of the future foot position. On the other hand, closer to heel-strike, the swing foot, which eventually becomes the stance foot, completely explains the next foot position – and the coefficients corresponding to the pelvis and other velocities go to zero in Figure S6.

We repeated the regressions with other foot markers for foot position or one of the pelvis markers for pelvis position, and the results were qualitatively similar.

These remarks come with the caveat that because of the possible correlations between the swing foot state and pelvis state, the inferred coefficients likely have greater error bars and could change with small changes in the model. Given the possibility of correlated inputs, note that there is no a priori necessity that the natural variability is sufficient excitation of the system to be able to infer the linear relations we seek. While we have considered different sets of explanatory variables for the foot position, we did not use formal methods to reduce the space of inputs: for instance, we could compute the principal components of the input covariance and use

a smaller number of input variables that are weighted combinations of the original input variables and capture most of the input variance. Such input correlations may automatically get reflected in larger error estimates for the corresponding coefficients, as inferred by bootstrap statistics. Alternatively, we could systematically remove variables in a step-down regression based on variance fraction explained.

Remarks on the partial derivative notation and terminology. Throughout this article, we use the partial derivative notation to indicate sensitivities (regression coefficients), instead of indexed matrix elements like $J_{(1,1)}$, so as to clearly indicate what the input and output variables are. Nevertheless, we should remember that these are not true partial derivatives, but just statistical estimates of the partial derivatives based on a regression using particular subset of the full state of the system (and based on further assumptions about the nature of noise and how this noise propagates through the system). As we have seen in the preceding paragraphs, and especially in Figures S7, S5, and S6, the estimates of these so-called partial derivatives depend on the set of variables used as explanatory variables.

Our interpretation of the partial derivatives in Figures S4 is as how the next foot position is explained by just the pelvis — that is, as a linear predictive model. On the other hand, acknowledging that numerous relevant body state variables are still missing, the partial derivatives in Figure S6, which considers more explanatory variables, try to capture the evolution of the whole system having already incorporated any foot position dynamics.

Key events during a step: Mid-stance, push-off and heel-strike denotations. The phase $\phi = 0$ is the mid-stance of a given step, as defined in the main manuscript. In Figure 2b-d of the main manuscript and Figures S4-S9, we have two vertical red lines, one solid, one dashed, which respectively correspond to moments just after push-off and just before heel-strike. Because we did not have force measurements, we used kinematic definitions for these events. The red lines correspond to averages over all strides and all trials, and is meant as an approximate indicator of when the step-to-step transition happens. The just-before-heel-strike line is at $\phi = 0.22$ and the just-after-push-push-off is at $\phi = 0.36$. The just-before-heel-strike moment was defined as the moment when the swing leg changes velocity direction from forward to backward relative to the pelvis (averaged over all trials). The just-after-push-off moment was defined as the moment when the stance leg changes velocity direction from backward to forward relative to the pelvis (averaged over all trials).

Note that we define a different ϕ variable for each and every stance phase, with $\phi = 0$ at its mid-stance. Therefore, from the perspective of a given step's mid-stance, $\phi = 0.5$ and $\phi = -0.5$ are only 'approximately' the next and previous mid-stances of the contralateral leg, and not exactly those mid-stances. This is because the step length varies from step to step, so the next mid-stance will not be exactly at $Y_{\text{pelvis}} = D_{\text{stride}}/2$.

Remarks on walking speeds used. For incidental reasons not part of explicit protocol design, we used two different treadmills, one for subjects 1-5 and another for subjects 6-10. Because of the treadmills' different speed control features, slightly different walking speed sets were used for the two subject groups, as noted in the main manuscript.

Remarks on a short trial. While 29 out of the 30 trials (10 subjects $\times$ 3 speeds each) had over 220 strides each (averaging 265 strides), exactly one trial was much shorter and had only 125 strides of usable data. We did not remove results from this shorter trial from any of the results presented and results from this shorter trial were not significantly different from the overall distribution across subjects.

Treadmills with different widths and lengths do not affect foot placement dynamics. The two treadmills had substantially different widths (0.92m versus 0.51m) and somewhat different lengths (1.52m versus 1.27m). However, as shown in Figure S1, we did not observe significant differences in the Jacobian elements between these two treadmill-subject groups. The similarity of the coefficients despite considerable difference in treadmill widths suggests that keeping away from treadmill limits were not a concern, with the caveat that we did not explicitly control for subject properties or treadmill lengths. See also Figure S11, which shows that typical walking behavior of the subjects, generally remaining far away from the treadmill limits.

Pelvic markers versus center of mass. For an average standing human, the center of mass is close to height of the navel, about 54-56% of a person's height, and roughly at the level of the Posterior Superior Iliac Spine

[6]. Our three pelvis markers were roughly located at this height, two markers placed symmetrically on the back and one on the front. A weighted average of these markers gives a point inside the body approximating the standing center of mass. This weighted-average point remains a reasonable approximation of the center of mass as a person walks, but, as a person walks or otherwise changes the shape of their body, the center of mass moves around relative to the body segments, so that no single anatomical position can track the center of mass exactly [6]. Of course, individual anatomical variation also precludes from this weighted average of markers being an exact center of mass estimate even while standing; we did not explicitly compare the location relative to a measured center of mass. In this article, we do not explicitly use the fact that the effective pelvis position is close to the center of mass, but the explanatory power of the pelvis state for walking dynamics is likely due to its being a reasonable approximation of the center of mass. Thus, we intend this pelvis position as a proxy for the center of mass, analogous to using a point-mass model for the upper body, as has been successfully employed in many locomotion studies (e.g., [7]). Also, in the main manuscript, while we use the term 'pelvis' as a short-hand for this weighted average of markers, the markers were at the upper end of the pelvis, lower part of the torso, and close to the height of the navel; hence our use of the term 'upper body' in the title.

Specialness of the mean trajectory. Because our regression equations are linear mappings from and to deviations from 'average', it may superficially appear that our method assumes that the average measured trajectories of both the pelvis and the foot are somehow special. However, in a certain formal sense, we do not explicitly assume such specialness, described as follows with an example.

Say, we have noisy data relating variables p and q. First, we posit a general linear (affine) relation $p = A_1 q + B_1$ and use an ordinary least squares calculation on p and q to estimate A_1 and B_1. Clearly, this affine relation gives no special meaning to the means p^* and q^* of p and q respectively. Next, positing linear relations between deviations about the mean $(p - p^*) = A_2(q - q^*) + B_2$, we perform a separate ordinary least squares calculation, now on $(p - p^*)$ and $(q - q^*)$, to get A_2 and B_2. It can be proven that the obtained regressions are equivalent, in that we are mathematically guaranteed to obtain $A_1 = A_2$ and $B_1 = p^* - A_2 q^* + B_2$. This is true of ordinary least squares regression. Thus, just inferring mappings between deviations from means need not give any special meaning to the mean.

Of course, if there is significant non-linearity of the dynamical system and the noise is substantially non-Gaussian, the mean motion of the perturbed dynamical system may be slightly different from that of the unperturbed motion of the system, and ordinary least squares or even linear relations may not be appropriate any longer.

Nevertheless, it is conceivable that the human walking controller actively reduces deviations from a special trajectory. There is evidence that at least some aspects of human locomotion (especially average trajectories) can be predicted by metabolic energy minimization (e.g., [7, 8]), so perhaps this special trajectory is predicted by such energy optimality. On the other hand, there are some situations in which it is not immediately clear if indeed the nervous system tries to achieve such a special "target" motion aggressively, optimal or otherwise, as perhaps (e.g., variability in speed-position on treadmill or in other mechanically unimportant control manifolds [9, 10]). At least in this article, we remain agnostic about the optimality of motion that the nervous system tries to achieve overall.

Linearity of dynamics and control. Here, we have assumed linearity of the various relations, which seems appropriate given that the natural variability explores only a small neighborhood of the average trajectory. Also, a linear model has smaller number of parameters than a general quadratic function, and therefore could be estimated with greater confidence with limited data. Because of its simplicity, such linear controllers or their variants abound in the world of mathematical models of locomotion controllers, whether for foot placement or joint torque control or modulation of other control parameters. e.g., [11, 12, 13, 14, 15, 16, 17, 18, 19, 4, 20, 21, 22, 23, 24]. As noted in the main manuscript, one of these posited foot-placement controllers for walking is the 'extrapolated center of mass model' of At Hof and others [17, 25, 12]. Unlike our general linear regression, the XcoM is a *particular* linear function of the sideways center of mass position and velocity: $X_{\text{com}} + \dot{X}_{\text{com}}/\omega_0$, where $\omega_0 = \sqrt{g/\ell_0}$, g is acceleration due to gravity, and ℓ_0 is a leg length for an equivalent inverted pendulum biped model. Using $g = 9.81$ ms^{-2} and $\ell_0 = 0.95$ m, we have $X_{\text{com}} + 0.31\dot{X}_{\text{com}}$, with same units convention as in our main manuscript. This linear function is similar to our equation in the main manuscript (equation

3.1), which we derived from data with fewer pre-assumptions about what variables were important; thus, the XcoM model could be considered a special case of our regression. Indeed, while XcoM model at heel-strike could explain about 45% of the sideways foot-placement (see Figure 8 of [25]), the more general regression from pelvis state at heel-strike could explain close to 89% of the sideways foot placement variance ($\phi = 0.35$ in figure 2b and 2c of main manuscript). Such explanation of a high fraction of foot placement variance could point to the promise of 'data mining' approaches such as ours in other contexts. Also, we remark that the XcoM model is often (at least superficially) described as the foot placement being dependent on the actual position and velocity of the center of mass, as opposed to our model in which we suggest that the foot placement might be dependent on deviations from some nominal trajectory; of course, these descriptions may sometimes be formally equivalent, as noted earlier. Finally, in contrast to the XcoM work, our interest in this article has mostly been the prediction of future foot placement from current or past body state, especially as early as the mid-stance previous to the foot placement.

References

[1] G. H. Golub and C. F. Van Loan. *Matrix computations*, volume 3. JHU Press, 2012.

[2] B. Efron. *The jackknife, the bootstrap and other resampling plans*, volume 38. SIAM, 1982.

[3] H. R. Kunsch. The jackknife and the bootstrap for general stationary observations. *The Annals of Statistics*, 17(3):1217–1241, 1989.

[4] S. Revzen and J. M. Guckenheimer. Finding the dimension of slow dynamics in a rhythmic system. *J. Roy. Soc. Interface*, 9:957–971, 2012.

[5] T. Nakamura and M. Small. Small-shuffle surrogate data: Testing for dynamics in fluctuating data with trends. *Phys. Rev. E*, 72(5):056216, 2005.

[6] S. A. Gard, S. C. Miff, and A. D. Kuo. Comparison of kinematic and kinetic methods for computing the vertical motion of the body center of mass during walking. *Human movement science*, 22(6):597–610, 2004.

[7] M. Srinivasan. Fifteen observations on the structure of energy minimizing gaits in many simple biped models. *J. Roy. Soc. Interface*, 8:74–98, 2011.

[8] R. McN. Alexander. *Principles of animal locomotion*. Princeton University Press, Princeton., 2003.

[9] J. B. Dingwell, J. John, and J. P. Cusumano. Do humans optimally exploit redundancy to control step variability in walking? *PLoS computational biology*, 6(7):e1000856, 2010.

[10] N. J. Rosenblatt, C. P. Hurt, M. L. Latash, and M. D. Grabiner. An apparent contradiction: increasing variability to achieve greater precision? *Experimental brain research*, 232(2):403–413, 2014.

[11] R. M. Ghigliazza, R. Altendorfer, P. Holmes, and D. Koditschek. A simply stabilized running model. *SIAM Review*, 47:519–549, 2005.

[12] A. L. Hof, S. M. Vermerris, and W. A. Gjaltema. Balance responses to lateral perturbations in human treadmill walking. *J. Exp. Biol.*, 213:2655–2664, 2010.

[13] A. D. Kuo. Stabilization of lateral motion in passive dynamic walking. *Int. J. Robot Res.*, 18:917–930, 1999.

[14] J. H. Solomon, M. Wisse, and M. J. Z. Hartmann. Fully interconnected, linear control for limit cycle walking. *Adaptive Behavior*, 18:492–506, 2010.

[15] J.E. Seipel and P. Holmes. Running in three dimensions: Analysis of a point-mass sprung-leg model. *Int. J. Robotics Research*, 24:657–674, 2005.

[16] M. A. Townsend. Biped gait stabilization via foot placement. *Journal of biomechanics*, 18(1):21–38, 1985.

[17] A. L Hof, R. M. van Bockel, T. Schoppen, and K. Postema. Control of lateral balance in walking: experimental findings in normal subjects and above-knee amputees. *Gait & posture*, 25(2):250–258, 2007.

[18] H. Geyer and H. M. Herr. A muscle-reflex model that encodes principles of legged mechanics produces human walking dynamics and muscle activities. *IEEE Trans Neural Syst Rehabil Eng*, 18:263–273, 2010.

[19] P. A. Bhounsule, J. Cortell, A. Grewal, B. Hendriksen, J. G. Daniël Karssen, C. Paul, and A. Ruina. Low-bandwidth reflex-based control for lower power walking: 65 km on a single battery charge. *The International Journal of Robotics Research*, 33(10):1305–1321, 2014.

[20] H. Miura and I. Shimoyama. Dynamic walk of a biped. *The International Journal of Robotics Research*, 3(2):60–74, 1984.

[21] J. M. Wang, D. J. Fleet, and A. Hertzmann. Optimizing walking controllers. In *ACM Transactions on Graphics (TOG)*, volume 28, page 168. ACM, 2009.

[22] K. Yin, K. Loken, and M. van de Panne. Simbicon: Simple biped locomotion control. In *ACM Transactions on Graphics (TOG)*, volume 26, page 105. ACM, 2007.

[23] H. Hemami and C. L. Golliday Jr. The inverted pendulum and biped stability. *Mathematical Biosciences*, 34(1):95–110, 1977.

[24] M. Maus, S. Revzen, and J. Guckenheimer. Drift and deadbeat control in the floquet structure of human running. In *Conference on Dynamic Walking*, 2012.

[25] A. L. Hof. The extrapolated center of mass concept suggests a simple control of balance in walking. *Human movement science*, 27:112–125, 2008.

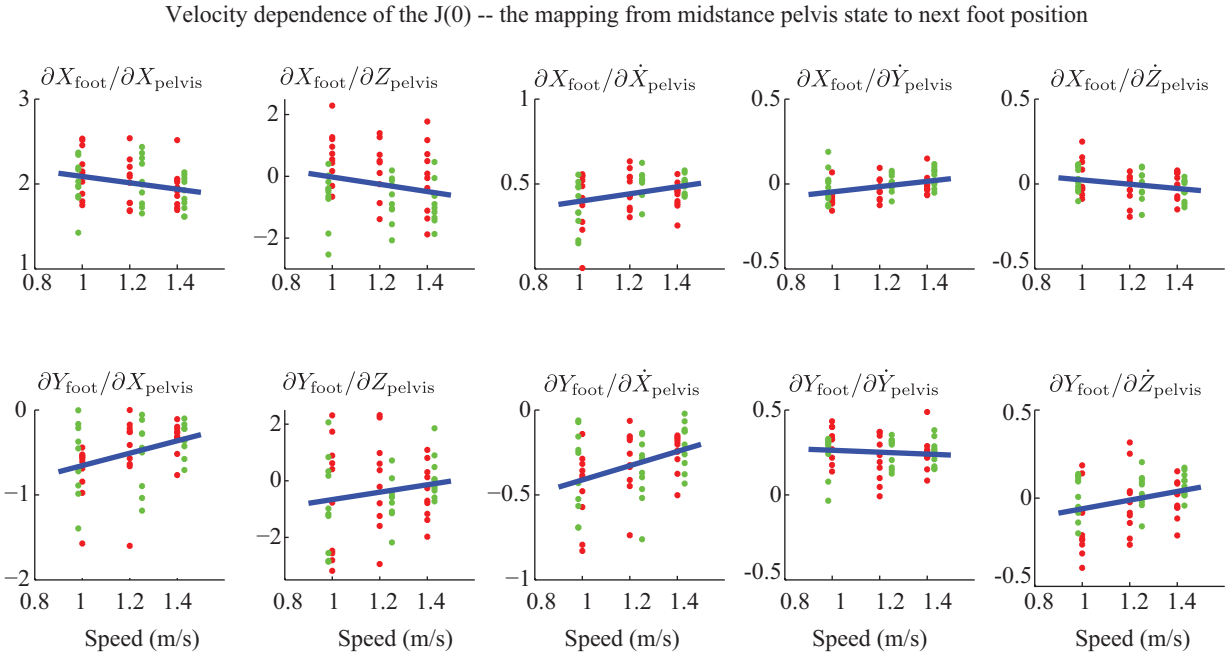

Figure S1: Speed and treadmill dependence of the $J(0)$. This figure shows the inferred best-fit coefficients $J(0)$ for each of the 30 trials, same as those in Figure 2a of the main manuscript, plotted against the treadmill speed. The red dots indicate subjects 1-5 (treadmill 1, width 0.92m, length 1.52m) and the green dots indicate subjects 6-10 (treadmill 2, width 0.51m, length 1.27m). The coefficients do not show obvious or substantial speed dependence; the best-fit linear function of speed explains only a small fraction of the variance in the coefficients. Also, the coefficients were not significantly different between the two treadmills and subject groups.

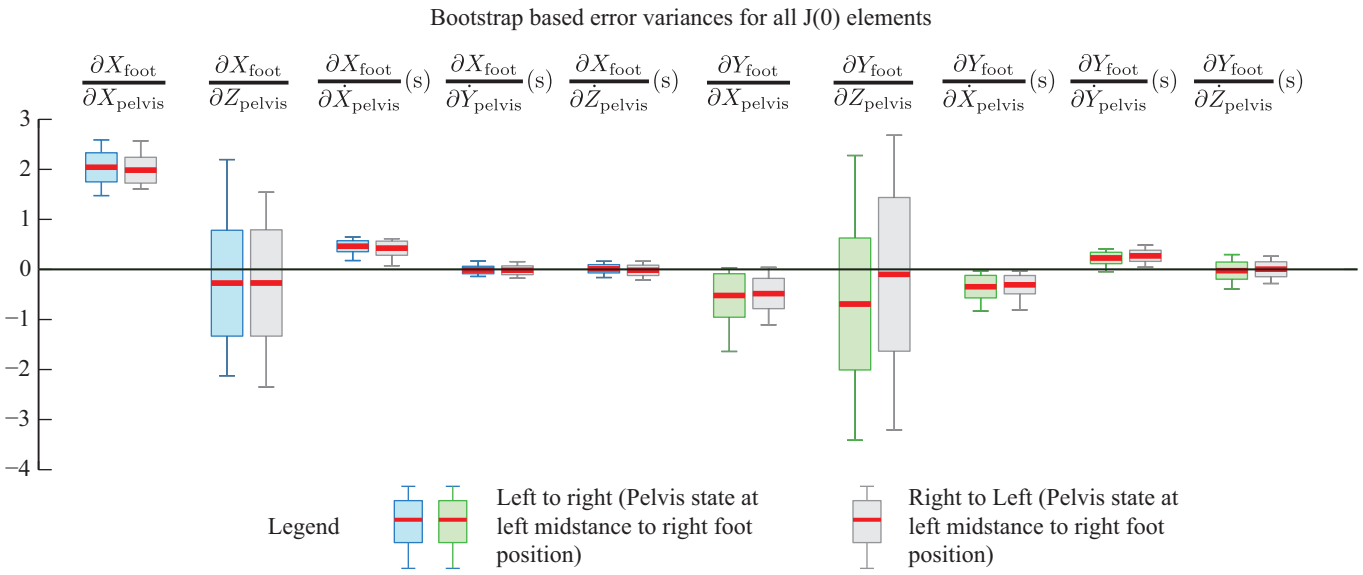

Figure S2: Pooled bootstrap distributions of $J(0)$. This figure is similar to Figure 2a of the main manuscript, except the standard deviations shown here are obtained using from bootstrap statistics. The bootstrap distributions were obtained separately for each trial and subject separately, and then all the bootstrap distributions are pooled to get the distribution for each coefficient. The standard deviations of these pooled distributions are shown in this figure. Compare these standard deviations to the standard deviations from inter-subject and inter-trial variability of the best fit coefficients, depicted in Figure 2a of the main manuscript.

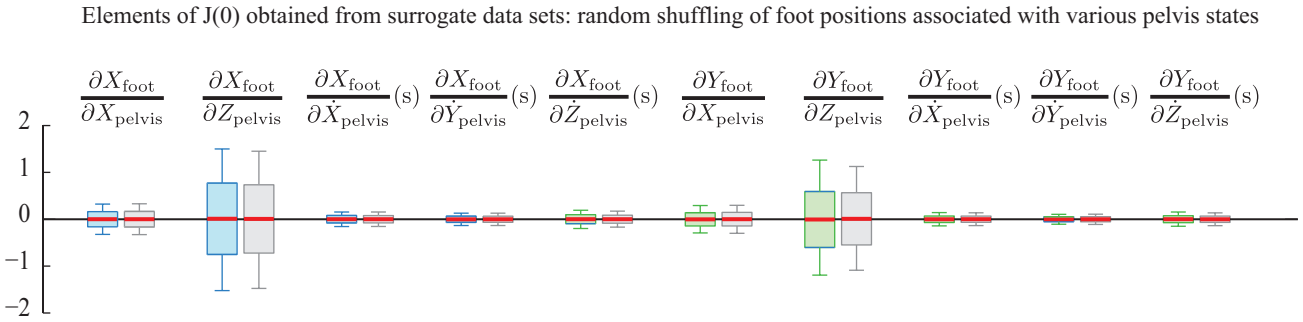

Figure S3: Distribution of $J(0)$ from shuffled surrogate data sets. Distribution of $J(0)$ elements obtained from surrogate data sets, which have the pelvis-foot-state associations shuffled through re-sampling. We see that the distributions are centered around zero, as should happen due to shuffling. Comparing these distributions to those in Figure 2a of the main manuscript and Figure S2, we see that the extent of the 95% confidence intervals from surrogate data are bounded away from the mean best estimates of of the significantly non-zero coefficients of Figure 2a. That is, the probability of such surrogate data generating any one of the coefficients deemed non-zero in Figure 2a is less than 0.05. ($p < 0.05$).

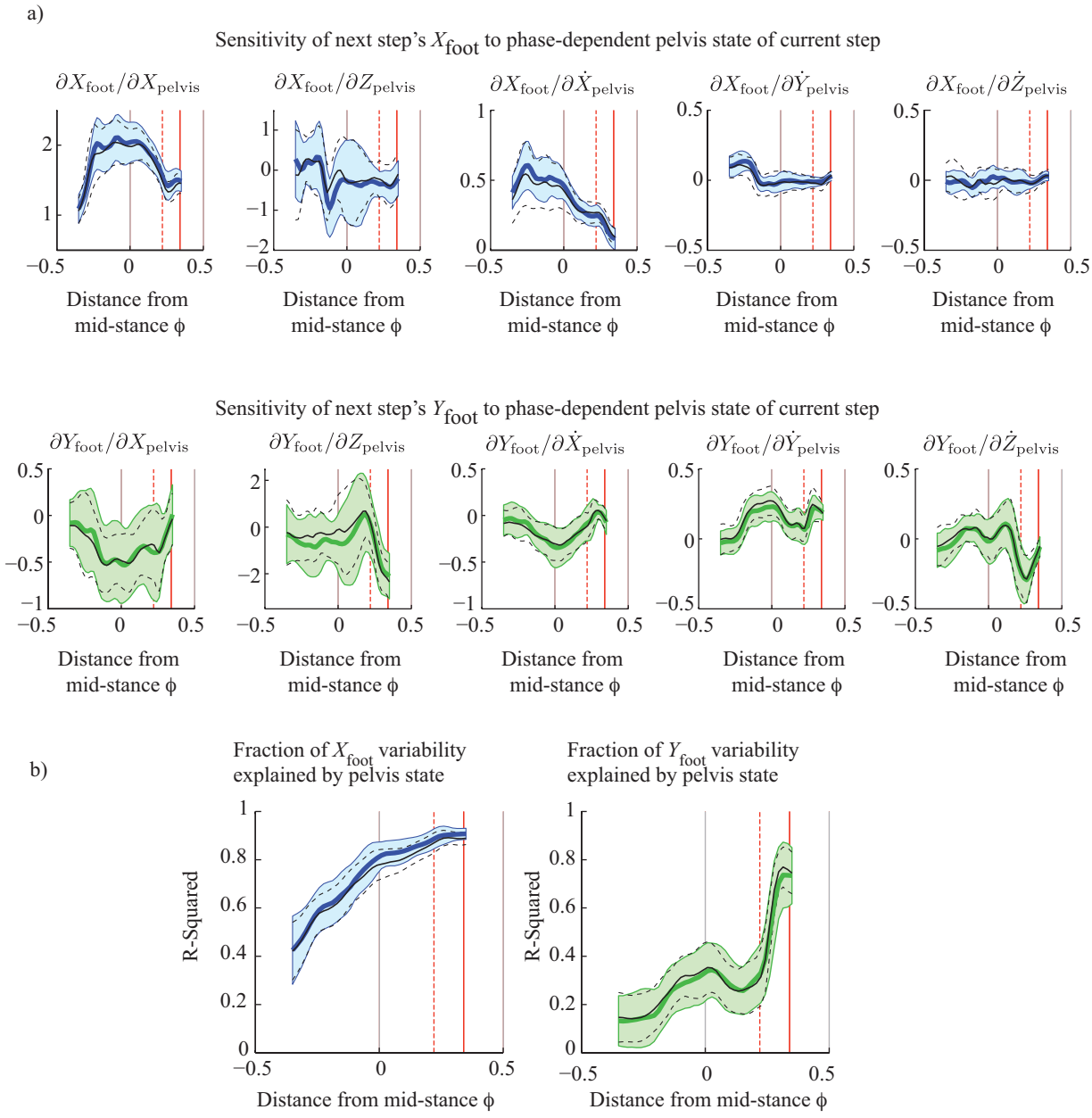

Figure S4: Linear relation from pelvis state to next stance foot position. This is the full version of the Figure 2b and 2c of the main manuscript, showing the phase dependence of all the regressed coefficients. a) The regression was from the the pelvis state $P(\phi)$ as the input to the foot position $(X_{\text{foot}}, Y_{\text{foot}})$ as the output: 5 input variables and 2 output variables. b) The fraction of $(X_{\text{foot}}, Y_{\text{foot}})$ variability explained by pelvis state during the previous stance phase. We noticed that dropping the Z and $\dot{Z}$ regressors does not change the regressed coefficients for the other inputs significantly, suggesting that a lower-dimensional top-view model may be sufficient.

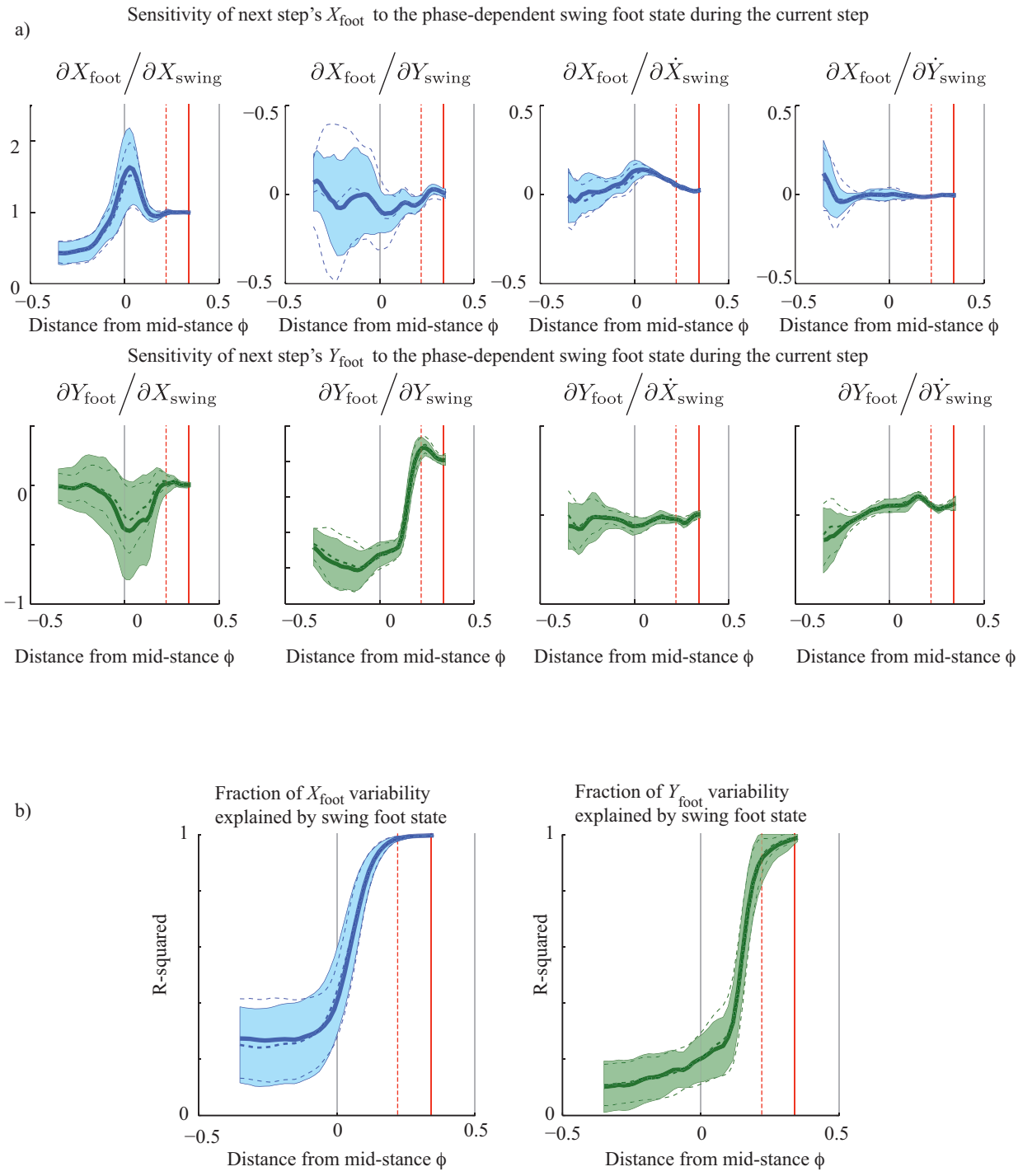

Figure S5: Linear relation from swing foot state to next stance foot position. a) The linear regression coefficients from the swing foot state $R(\phi) = (X_{\text{swing}}, \dot{X}_{\text{swing}}, Y_{\text{swing}}, \dot{Y}_{\text{swing}})$ to the foot position $(X_{\text{foot}}, Y_{\text{foot}})$. The regression consists of 4 input variables and 2 output variables. b) The fraction of $(X_{\text{foot}}, Y_{\text{foot}})$ variability explained by pelvis state during the previous stance phase. Adding the Z variables for the swing foot state do not change any of these results significantly. Panel-b of this figure has been integrated into Figure 2b of the main manuscript.

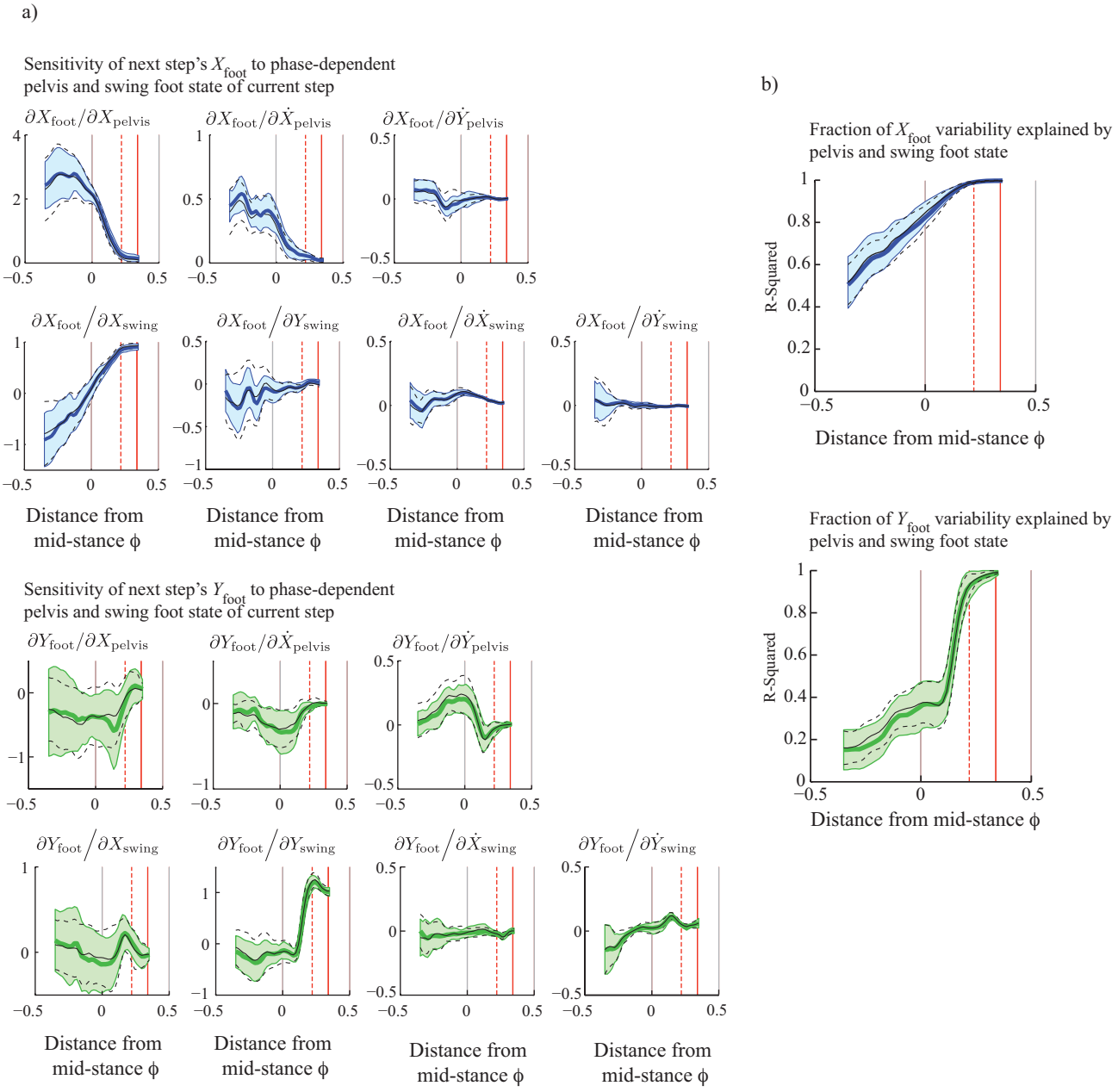

Figure S6: Linear relation from pelvis + swing foot state to next stance foot position. a) The linear regression coefficients from the 'full top-view state' at phase ϕ to the next foot position $(X_{\text{foot}}, Y_{\text{foot}})$. The pelvis and swing foot positions are measured relative to the current stance foot. The regression consists of 14 input variables and 2 output variables. b) The fraction of $(X_{\text{foot}}, Y_{\text{foot}})$ variability explained by pelvis state during the previous stance phase. Note that the corresponding coefficients are dramatically different from those in figures S4 and S5, because of correlations between the regressors, in particular, the pelvis state and the swing state.

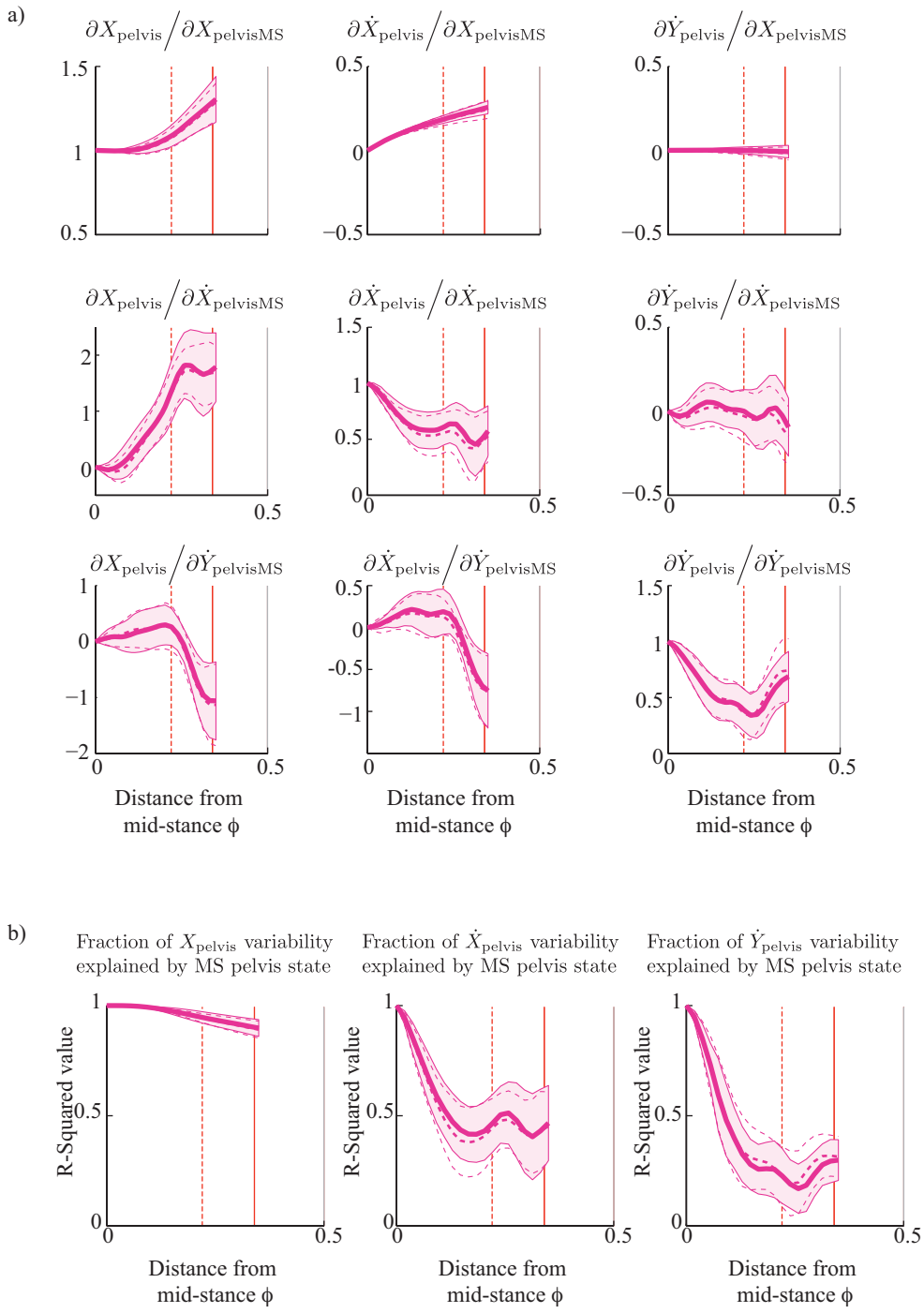

Figure S7: Linear relation from mid-stance pelvis state to future pelvis state. a) The linear regression coefficients from the mid-stance pelvis state $P(0)$ as input to future pelvis state $P(\phi)$ ($\phi > 0$); only top-view variables are considered so that he regression consists of 3 input variables and 3 output variables. b) The fraction of pelvis state $P(\phi)$ variability explained by mid-stance pelvis state $P(0)$. Using 3D pelvis states instead of 2D (i.e., including Z) does not improve the R-squared values.

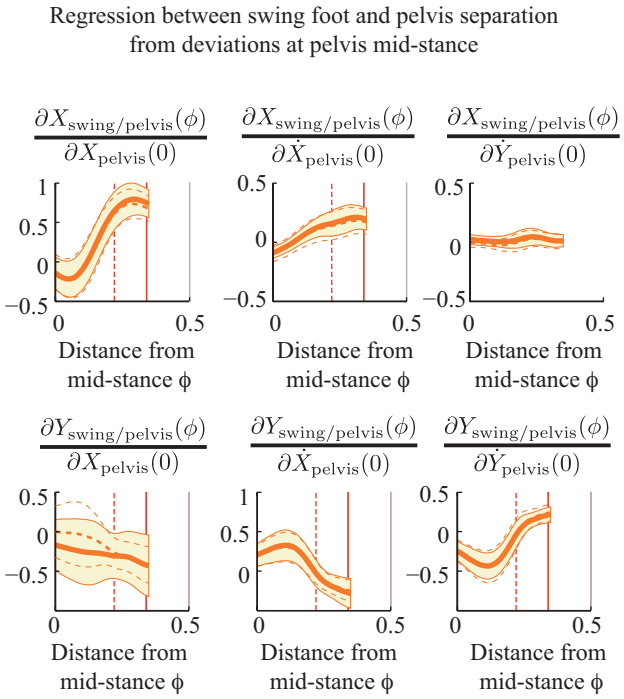

Figure S8: Linear relation from mid-stance pelvis deviation to future swing-foot-pelvis separation. The linear regression coefficients from mid-stance pelvis state $P(0)$ to the swing foot position relative to the pelvis $(X_{\text{swing/pelvis}},\ Y_{\text{swing/pelvis}})$, where $X_{\text{swing/pelvis}} = X_{\text{swing}} - X_{\text{pelvis}}$ and $Y_{\text{swing/pelvis}} = Y_{\text{swing}} - Y_{\text{pelvis}}$. We see that $\partial X_{\text{swing/pelvis}}/\partial X_{\text{pelvis}}(0)$ and $\partial X_{\text{swing/pelvis}}/\partial \dot{X}_{\text{pelvis}}(0)$ starts from a slightly negative value to become about 0.6 and 0.3 respectively by about heel-strike. This means that a positive mid-stance pelvis deviation $\Delta X_{\text{pelvis}}(0)$ or $\Delta \dot{X}_{\text{pelvis}}(0)$ will result in monotonically increasing deviation of the swing-foot-pelvis separation as ϕ increases. Note that this is a subtle idea — we are claiming additional deviation over and above the mean swing-foot-pelvis separation.

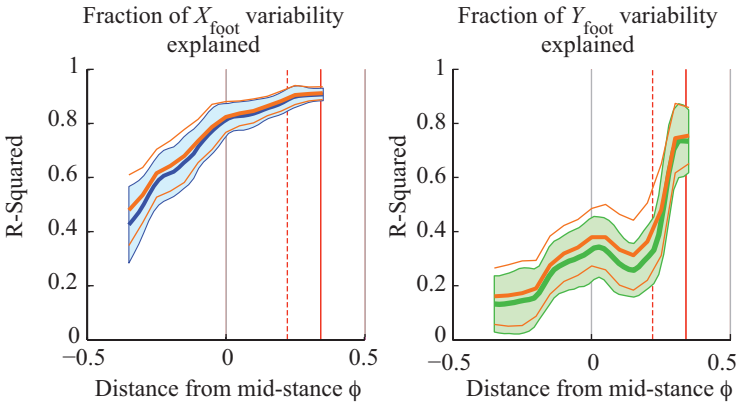

Figure S9: Station-keeping: Absolute position does not improve foot placement prediction. Comparison of R^2 values for regressions of pelvis state to next foot position, without and with the additional regressor of the absolute stance foot position. The blue and green curves and bands are identical to those in Figure 2a of the main manuscript and Figure S4, indicating the variance explained by pelvis state $P(\phi)$ alone. The overlaid orange curves are the R^2 values from adding the stance foot position. Note that these mean orange lines lie well within the 1 sd band of the pelvis-state-only regression. While the stance foot position regressor has almost no effect on the pelvis X_{foot}, the stance foot position has a small predictive effect on Y_{foot}, but still less than 5% increase in R^2 values.

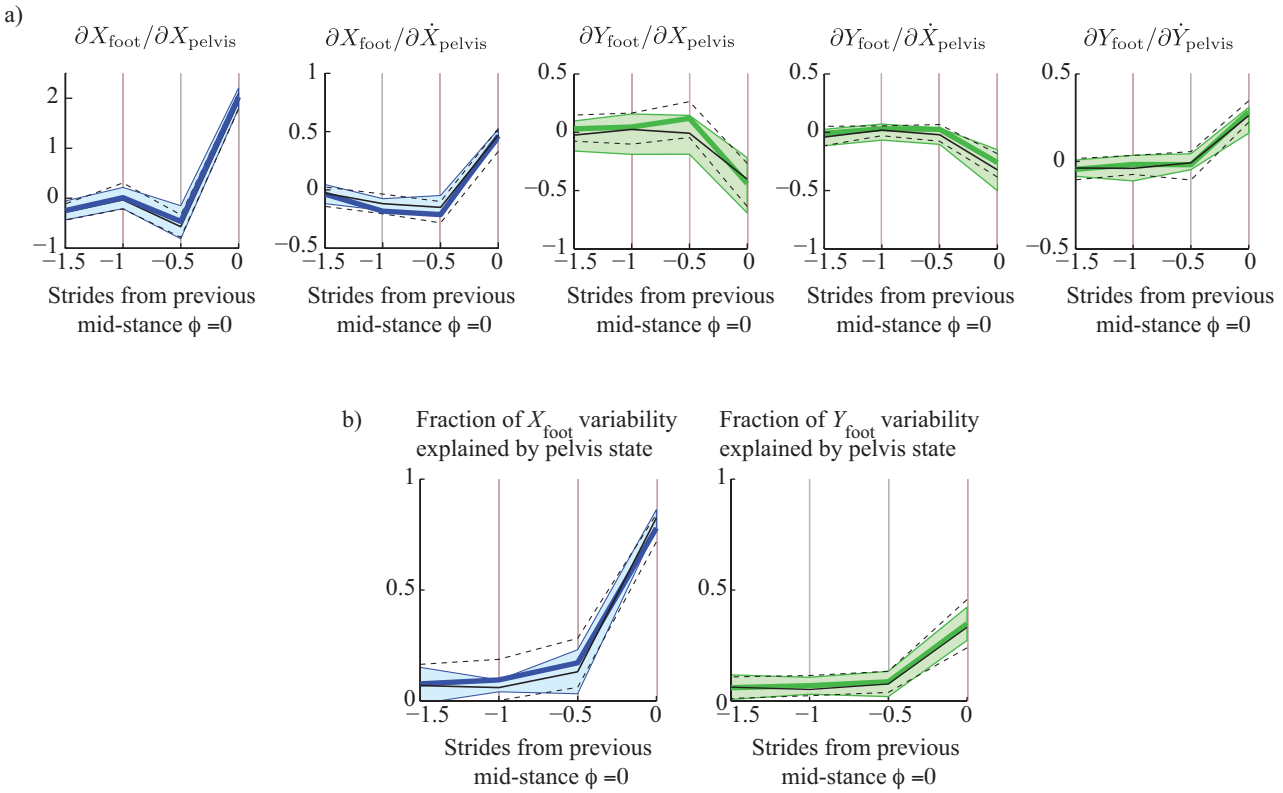

Figure S10: Previous strides cannot predict foot position as well. a) We performed regressions from the pelvis state $P(\phi)$ at the previous few mid-stances as the input to the foot position $(X_{\text{foot}}, Y_{\text{foot}})$ as the output. For a given output foot position (say, left foot), the mid-stance 0 denotes the previous contralateral mid-stance ($\phi = 0$, right foot stance) as in the rest of the article, -0.5 denotes the previous ipsilateral mid-stance (left foot stance), -1 denotes the contralateral mid-stance but from the previous stride (right foot stance), and -1.5 denotes the ipsilateral mid-stance from the previous stride (left foot stance). In this calculation, all mid-stance states are defined and measured from the stance foot of that step. The significant coefficients quickly approach zero as we consider mid-stances further in the past. b) We see that the fraction of lateral foot position drops from about 81% from the immediately previous mid-stance (mid-stance 0) to about 13% if we use the previous mid-stance (mid-stance -0.5, ipsilateral mid-stance of previous stride). The R^2 values are not significantly above zero while using mid-stance states from even previous steps (-1 and -1.5).

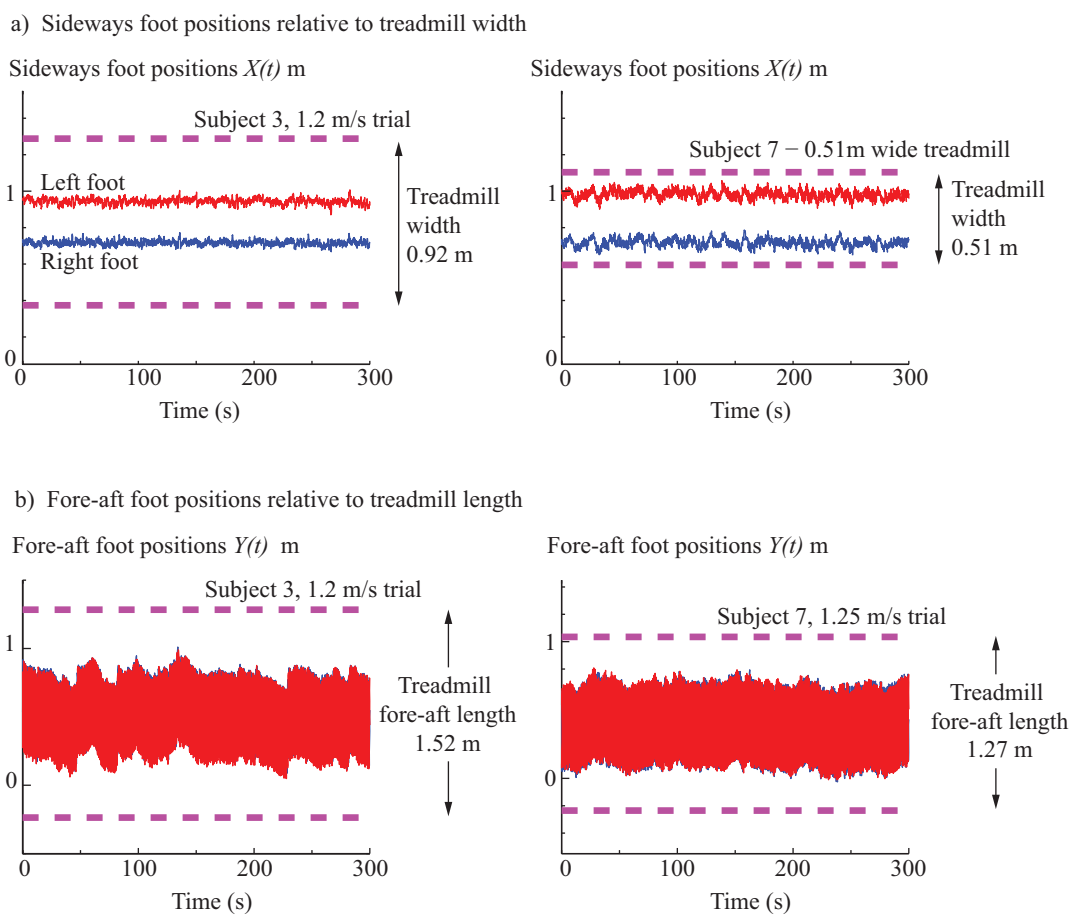

Figure S11: Subjects stayed far away from treadmill limits. a) The 'absolute' sideways position $X(t)$ of the left and right foot is shown as a function of continuous time over a whole trial. Two subjects are shown, subject 3 and subject 7, remaining generally away from the respective treadmill limits. b) The 'absolute' fore-aft position of the left foot is shown (right foot plot is underneath this graph, therefore obscured). The left foot's fore-aft excursion is much smaller than the full length of the treadmill. All subjects generally kept away from the treadmill edges in all trials, except perhaps occasionally wandering closer to an edge once or twice during a whole trial.

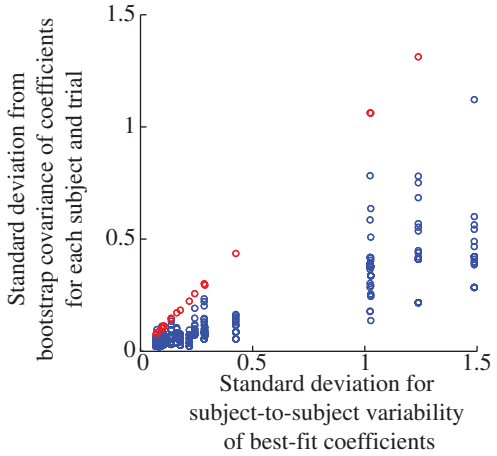

Figure S12: Inter-subject variability versus intra-trial error estimate for each coefficient. We hypothesized that the bootstrap error estimate (standard deviation) will be higher for those coefficients for which the best estimate show greatest inter-subject variability. Here, we plot the standard deviation of the subject-trial-variability for each coefficient versus the boot-strap error estimate for that coefficient for all subject trials (blue circles); we do see that the coefficients that have high inter-subject variability also have higher error estimate for each trial, but this relation is not 1:1 (red circles). The different coefficients have different units, some having no units and some having units of s^{-1}. The regression considered here is the same as that in figures S1-S2.